Renewable Energy 147 (2020) 895–902

Contents lists available at ScienceDirect

Renewable Energy

journal homepage: www.elsevier.com/locate/renene

Description of short circuit current of outdoor photovoltaic modules by multiple regression analysis under various solar irradiance levels

Koichi Nakayama [a], Masaki Tsuji [a], Jakapan Chantana [a, b, *], Yu Kawano [a], Takahito Nishimura [c], Yoshihiro Hishikawa [d], Takashi Minemoto [a, **]

[a] Department of Electrical and Electronic Engineering, Ritsumeikan University, 1-1-1 Nojihigashi, Kusatsu, Shiga 525-8577, Japan
[b] Research Organization of Science and Technology, Ritsumeikan University, 1-1-1 Nojihigashi, Kusatsu, Shiga 525-8577, Japan
[c] Ritsumeikan Global Innovation Research Organization, Ritsumeikan University, 1-1-1 Nojihigashi, Kusatsu, Shiga 525-8577, Japan
[d] National Institute of Advanced Industrial Science and Technology (AIST), Research Center for Photovoltaics, Tsukuba, Ibaraki 305-8568, Japan

ARTICLE INFO

Article history:
Received 2 June 2019
Received in revised form
10 September 2019
Accepted 16 September 2019
Available online 17 September 2019

Keywords:
Short-circuit current
PV module irradiance sensor
Solar irradiance levels
Multiple regression analysis

ABSTRACT

Short-circuit current (I_{SC}) values of test photovoltaic (PV) modules, i.e., multi-crystalline silicon, heterostructure-with-intrinsic-thin-layer, single-crystalline silicon back-contact, $CuInSe_2$ (CIS), and CdTe modules, are descripted using multiple regression analysis based on environmental factors (solar irradiance, average photon energy (APE), and module temperature (T_{mod})) under several solar irradiance levels. The APE is an index of the solar spectral irradiance distribution. PV module irradiance sensor (PVMS), single-crystalline silicon PV module, is used to investigate simultaneous solar irradiance ($IrrT_{PVMS}$). It is disclosed that I_{SC} is primarily determined by $IrrT_{PVMS}$. Error between the estimated I_{SC} and measured I_{SC} of test PV modules is investigated. Consequently, precise I_{SC} description (low error) is obtained when $IrrT_{PVMS}$ is utilized. The more precise description of the I_{SC} for CIS and CdTe PV modules, having the bandgap (E_g) different from PVMS, is realized when adding APE environment factor even under low $IrrT_{PVMS}$ ($\geq$0 kW/m^2), accumulated on both sunny day and cloudy day suggesting the enhancement of investigation opportunity. This is because APE minimizes spectral mismatch error caused by E_g difference between PVMS and test PV module. Moreover, the precision of I_{SC} description is further increased under enhanced $IrrT_{PVMS}$ of $\geq$0.5 kW/m^2 (on sunny day) due to stable solar irradiance.

1. Introduction

Solar energy, provided by photovoltaic (PV) modules, is one of the interesting alternative energies [1,2]. It is essential to investigate the performance of PV modules for the credibility of the technology after their fabrication. There are two ways to evaluate the performance of PV modules, which are power rating and energy rating. For the power rating, the conversion efficiency (Eff.) of the PV modules is measured under standard test condition (STC), namely incident solar irradiance of 1 kW/m^2, AM 1.5G solar spectrum distribution, and module temperature (T_{mod}) of 25 °C [3,4]. However, the PV modules are installed at outdoor location, where the STC is hardly occurred. Therefore, the performance evaluation of PV modules at the outdoor site by the power rating is not easy under STC. The energy rating therefore plays a role in evaluating the performance of PV modules at the outdoor location, which is composed of the measurements of PV module characteristics and data sets of environmental factors [5]. The energy rating thus requires the actual data of the PV characteristics and environmental data, at which the modules are installed. The description of the outdoor performance of PV modules based on the environmental factors is consequently needed for the evaluation of performances of the PV modules using the energy rating method [6].

The outdoor performance of PV modules is generally influenced by environmental factors, namely solar irradiance, average photon energy (APE), and T_{mod} [6–12]. It is noted that APE is an indicator of solar spectral irradiance distribution [12]. The description of the outdoor performances of the PV modules based on the environmental factors is a difficult task because a data set of the

* Corresponding author. Department of Electrical and Electronic Engineering, Ritsumeikan University, 1-1-1 Nojihigashi, Kusatsu, Shiga 525-8577, Japan.
** Corresponding author.
E-mail addresses: re0091fv@ed.ritsumei.ac.jp (K. Nakayama), re0075eh@ed.ritsumei.ac.jp (M. Tsuji), jakapan@fc.ritsumei.ac.jp (J. Chantana), kawano@fc.ritsumei.ac.jp (Y. Kawano), nishi-tk@fc.ritsumei.ac.jp (T. Nishimura), y-hishikawa@aist.go.jp (Y. Hishikawa), minemoto@se.ritsumei.ac.jp (T. Minemoto).

https://doi.org/10.1016/j.renene.2019.09.083
0960-1481/

environmental factors on sunny day (high solar irradiance of >0.8 kW/m^2) is required for the high precision [13–16]. The outdoor measurement opportunity for the environmental factors on the sunny day is limited for the precise description of the outdoor performances. In this work, the method to precisely descript the outdoor performances under not only sunny day but also cloudy day (various solar irradiance levels) was developed, thereby enhancing the outdoor measurement opportunity. It was furthermore reported that the outdoor PV measurement with the high precision in a small range of ±1-±2% has been attained using the simultaneous solar irradiance examined by PV module irradiance sensor (PVMS) since the solar spectral irradiance (E) at the outdoor site always changes [17]. Hereafter, the simultaneous solar irradiance measured by PVMS is named $IrrT_{PVMS}$. Therefore, the $IrrT_{PVMS}$ in this work was observed with the fast measurement time of below 200 ms by PVMS, which is single-crystalline silicon (sc-Si) PV module.

Of all outdoor performances of the PV modules, short-circuit current (I_{SC}) is important and affected by solar irradiance, APE, and T_{mod} [18]. The description of I_{SC} of the PV modules in terms of solar irradiance, APE, and T_{mod} is examined under several solar irradiance levels. Multiple regression analysis is known as a statistic tool, enabling us to separately and quantitatively investigate how multiple independent variables are related to a dependent variable through partial regression coefficient (PRC) [19].

In this contribution, the description of I_{SC} of the different-type PV modules was therefore conducted to separately and quantitatively analyze how each environmental factor (solar irradiance (IrrT or $IrrT_{PVMS}$), APE, or T_{mod}) affects the I_{SC} under different solar irradiance levels by the multiple regression analysis. The solar irradiance called IrrT was examined by pyranometer with time response up to approximately 8 s. The IrrT and $IrrT_{PVMS}$ were used to descript the I_{SC} for the comparison. It will be later revealed that the more precise description of I_{SC} is attained, when the $IrrT_{PVMS}$ (simultaneous solar irradiance) is utilized. The estimated I_{SC} of the PV modules was moreover calculated based on the IrrT, $IrrT_{PVMS}$, APE, or T_{mod} and compared with the actual I_{SC} measured at the outdoor location under different solar irradiance levels, thereby leading to the description of the relationship between the outdoor performance, which is I_{SC}, of the different-type PV modules and environmental factors at the installed outdoor location, which are the IrrT, $IrrT_{PVMS}$, APE, or T_{mod}.

2. Experimental details

2.1. PV modules and measurement setup

In this work, the different-type PV modules, which are (1) sc-Si PV module, (2) multi-crystalline silicon (mc-Si) PV module, (3) heterostructure-with-intrinsic-thin-layer (HIT) PV module, (4) single-crystalline silicon back-contact (BC) PV module, (5) $CuInSe_2$ (CIS) PV module, and (6) CdTe PV module, were installed at Ritsumeikan University, Kusatsu-city, Shiga-prefecture in Japan (north latitude 34°58', and east longitude 135°57'). The detailed characteristics of the installed test PV modules are shown in Table 1. Their photovoltaic performances such as maximum power, I_{SC}, open-circuit voltage (V_{OC}), fill factor (FF), and Eff. of the test PV modules in Table 1 were obtained under STC (IEC 60904-4 with Class-A) by indoor precision measurements at National Institute of Advanced Industrial Science and Technology (AIST) [17,20]. The sc-Si PV module was used as PVMS, whereas the mc-Si, HIT, BC, CIS, and CdTe PV modules were the test PV modules.

The environmental factors (IrrT, $IrrT_{PVMS}$, APE, or T_{mod}) at the installed location were measured from July 1st, 2016 to June 30th, 2017 (one year) on everyday from 4:00 a.m. to 20:00 p.m. as follows. To examine the T_{mod}, the thermocouples were attached to the back side of all test PV modules. The IrrT, which is the integrated solar spectral irradiance, was observed by pyranometer (EKO MS-402) from 285 to 2800 nm recorded every 1 min, where its time response is up to approximately 8 s. The $IrrT_{PVMS}$ measured by PVMS is defined by the ratio of $I_{SC\text{-}Si\text{-}measured}$ to $I_{SC\text{-}Si\text{-}STC}$. The $I_{SC\text{-}Si\text{-}measured}$ is the I_{SC} of the sc-Si PV module (PVMS) measured at outdoor installation location with the measurement time of below 200 ms, while $I_{SC\text{-}Si\text{-}STC}$ of 5.37 A of the sc-Si PV module was measured under STC as seen in Table 1.

To demonstrate the impact of the solar spectral irradiance variations, it is useful to determine a parameter representing the extent to which a solar spectrum shifts to the red or the blue. It was reported that the APE is used as an indicator of solar spectral irradiance variations [12,21–24]. The APE value under AM 1.5G reference spectrum in the wavelength range of 350–1050 nm is 1.88 eV [12,23,24]. The APE values of over 1.88 eV and below 1.88 eV represent the blue rich solar spectrum and red rich solar spectrum, respectively [12,18,23–25]. Consequently, the solar spectral irradiance was observed from 350 to 1050 nm by spectro-radiometer (EKO MS-700). The value of APE was next calculated as the integrated solar spectral irradiance divided by the integrated photon flux density, as demonstrated [12,21–24]:

$$APE_{x-y}(eV) = \frac{\int_x^y E(\lambda)d\lambda}{q\int_x^y \Phi(\lambda)d\lambda} \quad \text{and} \quad \Phi(\lambda) = \frac{E(\lambda)}{E_{photon}(\lambda)} \tag{1}$$

where q (C), Φ (s^{-1} m^{-2} nm^{-1}), and E_{photon} (eV) are elementary charge, spectral photon flux density, and energy of single photon, respectively [12,21–24]. Unit of E is W m^{-2} nm^{-1}, where E denotes the solar spectral irradiance determined from photon flux. The λ denotes wavelength. In this work, the *x* and *y* in Equation (1) are set to be from 350 to 1050 nm due to the limitation of the measuring instrument.

2.2. Models for description of I_{SC} of test PV modules

To descript the I_{SC} of the different-type test PV modules in terms of environmental factors (IrrT, $IrrT_{PVMS}$, APE, or T_{mod}), we proposed four models, called models A, B, C, and D, using the multiple regression analysis. The multiple regression analysis enables us to investigate how multiple independent variables are related to a dependent variable [19]. In this work, the environmental factors, which are multiple independent variables, are IrrT, $IrrT_{PVMS}$, APE, and T_{mod}, while the outcome, which is a dependent variable, is the I_{SC} of the test PV modules. For models A (IrrT) and B ($IrrT_{PVMS}$), the I_{SC} is described by IrrT in Equation (2) and $IrrT_{PVMS}$ in Equation (3), respectively, using the multiple regression analysis as shown:

$$I_{SC} = a \times IrrT \tag{2}$$

$$I_{SC} = b \times IrrT_{PVMS} \tag{3}$$

where *a* and *b* constants denote PRC, which are slopes of the regression lines for IrrT and $IrrT_{PVMS}$, respectively. For model C ($IrrT_{PVMS}$, and APE), the I_{SC} is described by $IrrT_{PVMS}$ and APE in Equation (4) as demonstrated:

$$I_{SC} = b \times IrrT_{PVMS} + c \times APE + e \tag{4}$$

where the *c* constant represents PRC, which is slope of the regression line for APE, and *e* is a constant. In addition, for model D ($IrrT_{PVMS}$, APE, and T_{mod}), the I_{SC} is described in terms of $IrrT_{PVMS}$,

Table 1
The detailed characteristics of the PV modules (sc-Si (PVMS), mc-Si, HIT, BC, CIS, and CdTe PV modules) installed at Ritsumeikan University, Kusatsu-city, Shiga-prefecture in Japan (north latitude 34°58', and east longitude 135°57'). Photovoltaic performances such as maximum power, short-circuit current (I_{SC}), open-circuit voltage (V_{OC}), fill factor (FF), and conversion efficiency (Eff.) of the PV modules were obtained under STC.

	Module 1	Module 2	Module 3	Module 4	Module 5	Module 6
Module Type	sc-Si	mc-Si	HIT	BC	CIS	CdTe
Manufacturer	SHARP	KYOCERA	Panasonic	SunPower	Solar Frontier	First Solar
Product Name	NT-84L5H	KC32T-02	N244α	E20/327	SF-160S	FS-4100
Maximum Power (W)	87.7	33.23	244.4	323.0	161.5	97.8
I_{SC} (A)	5.37	2.005	5.98	6.38	2.066	1.534
V_{OC} (V)	22.28	21.77	52.7	64.9	112.8	88.9
Eff. (%)	13.8	12.6	19.1	19.8	13.6	13.1
FF	0.733	0.761	0.755	0.780	0.717	0.693
Module Area (m^2)	0.634	0.265	1.28	1.63	1.22	0.72
E_g (eV)	1.16	1.17	1.09	1.13	1.21	1.47
Temperature coefficient for I_{SC} (%/°C)	0.020	0.039	0.034	0.035	0.006	0.045

APE, and T_{mod} in Equation (5) as depicted:

$$I_{SC} = b \times IrrT_{PVMS} + c \times APE + d \times T_{mod} + e \quad (5)$$

where d constant shows PRC, which is slope of the regression line for T_{mod}. It is noted that if the PRC (a, b, c, or d) is zero, the I_{SC} is independent from IrrT, $IrrT_{PVMS}$, APE, or T_{mod}, respectively.

After the I_{SC} is described based on the environmental factors by models A, B, C, and D, the I_{SC} is estimated using PRC (a, b, c, and d) together with the environmental factors, which is named the estimated I_{SC}. The error is useful tool for determining the precision of models (A, B, C, and D). The error between the estimated I_{SC} and measured (actual) I_{SC} in the same type PV module is given by:

$$Error(\%) = \frac{estimatedI_{SC} - measuredI_{SC}}{measuredI_{SC}} \times 100(\%) \quad (6)$$

where the measured I_{SC} is the I_{SC} of the test PV modules measured at the outdoor location with the measurement time of below 200 ms. According to Equation (6), it allows us to understand and descript which model leads to the most accurate estimated I_{SC}, which is close to the measured (actual) I_{SC} of PV modules at outdoor site.

3. Results and discussion

3.1. Description of I_{SC} of test PV modules in terms of IrrT and $IrrT_{PVMS}$

It is considered that the I_{SC} is strongly influenced by solar irradiance as it is the integrated solar spectral irradiance. In this section, the models A (IrrT) and B ($IrrT_{PVMS}$) were therefore investigated in the test mc-Si, HIT, BC, CIS, and CdTe PV modules. According to the multiple regression analysis, the PRC values (a and b constants) for models A (IrrT) and B ($IrrT_{PVMS}$) were calculated under the environmental factor data set of solar irradiance ($\geq$0 kW/m^2) in one year. Table 2 shows the resulting PRC values (a and b constants) for models A and B of the test mc-Si, HIT, BC, CIS, and CdTe PV modules. It is seen that the PRC values (a and b constants) in Table 2 are higher than zero, implying that the I_{SC} is positively related to the IrrT and $IrrT_{PVMS}$. Moreover, the I_{SC} values of the test PV modules are zero at the IrrT and $IrrT_{PVMS}$ of zero. In Table 2, the b values of the test PV modules (1.999, 6.003, 6.435, 1.997, and 1.541 for mc-Si, HIT, BC, CIS, and CeTe, respectively) are closer to their I_{SC} under STC (2.005, 5.98, 6.38, and 2.066, and 1.534 A for mc-Si, HIT, BC, CIS, and CeTe, respectively in Table 1) than the a values. The result implied that the I_{SC} descripted by $IrrT_{PVMS}$ (model B) demonstrates the higher precision than that descripted by IrrT (model A). This is because the $IrrT_{PVMS}$ is observed using the sc-Si PV module (PVMS) with the fast measurement time of below 200 ms, whereas the IrrT is investigated utilizing pyranometer (EKO MS-402) with the much slower time response up to approximately 8 s. The fast measurement time is needed for the high precision because the solar spectral irradiance always changes at the outdoor site [17,26,27]. Moreover, angle of incident (AOI) of the sc-Si PV module is similar to that of the test PV module, while AOI of the pyranometer is different from that of the test PV modules.

Fig. 1 furthermore depicts the I_{SC} value as functions of (a) IrrT and (b) $IrrT_{PVMS}$ for the mc-Si PV module as well as the I_{SC} value as functions of (c) IrrT and (d) $IrrT_{PVMS}$ for the CdTe PV module. The solid lines represent the regression lines using the multiple regression analysis for IrrT (model A) and $IrrT_{PVMS}$ (model B), where the PRC values (a and b constants) are shown. The I_{SC} values of the mc-Si PV module and CdTe module are observed in Fig. 1 as examples of the investigation, because the bandgap (E_g) of the mc-Si PV module (1.17 eV) is the closest to that (1.16 eV) of the sc-Si PV module (PVMS), whereas the E_g (1.47 eV) of the CdTe PV module is the most different from that of the sc-Si PV module (PVMS) in Table 1. In Fig. 1(a) and (b), the regression lines for the I_{SC} of the mc-Si module as functions of IrrT and $IrrT_{PVMS}$ are illustrated with a and b constants of 1.849 and 1.999, respectively. It is obviously seen that the less scattering I_{SC} data along with the regression line for the I_{SC} as a function of $IrrT_{PVMS}$ in Fig. 1(b) is presented owing to the $IrrT_{PVMS}$ observed by the sc-Si PV module (PVMS) with the fast measurement time and the same AOI as previously explained. In addition, the scattering I_{SC} data in Fig. 1(d) for the CdTe PV module is more severe than that in Fig. 1(b), when I_{SC} is descripted by the $IrrT_{PVMS}$ (model B). This is because the E_g of CdTe in Table 1 is the most different from that of the sc-Si PV module (PVMS).

Fig. 2 additionally demonstrates the histograms of error (%) for the I_{SC} values of the test PV modules ((a) mc-Si, (b) HIT, (c) BC, (d) CIS, and (e) CdTe modules), where the I_{SC} is descripted by IrrT (model A) and $IrrT_{PVMS}$ (model B). The figures were constructed with 174,285 data points in a year with solar irradiance ($\geq$0 kW/m^2), accumulated on not only sunny day but also cloudy day. The

Table 2
The resulting PRC values (a and b constants) for models A and B of the test mc-Si, HIT, BC, CIS, and CdTe PV modules in Equations (2) and (3), respectively, under a year data with solar irradiance of $\geq$0 kW/m^2. The I_{SC} is descripted by the model A, and the model B.

PV module	mc-Si	HIT	BC	CIS	CdTe
a	1.849	5.557	5.961	1.869	1.428
b	1.999	6.003	6.435	1.997	1.541

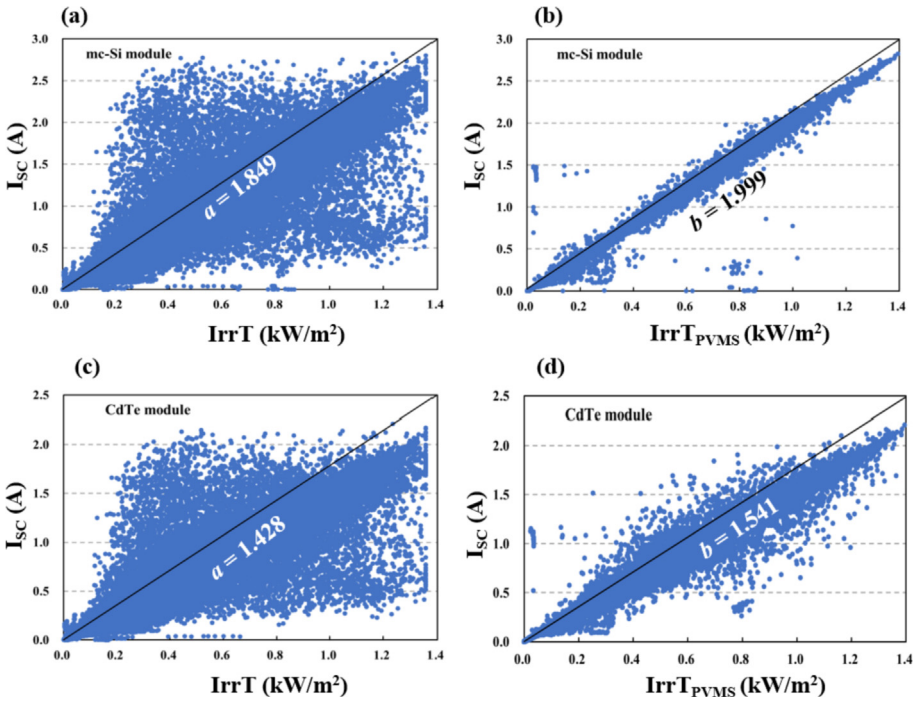

Fig. 1. I_{SC} value as functions of (a) IrrT and (b) $IrrT_{PVMS}$ for the mc-Si PV module, as well as the I_{SC} value as functions of (c) IrrT and (d) $IrrT_{PVMS}$ for the CdTe PV module under the data set in a year with solar irradiance of ≥0 kW/m^2. The solid lines represent the regression lines using the multiple regression analysis for IrrT (model A) and $IrrT_{PVMS}$ (model B), where the PRC values (*a* and *b* constants) are shown.

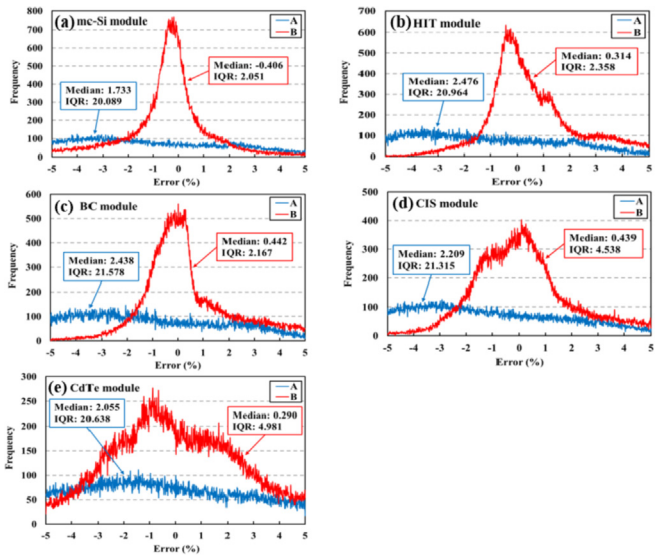

Fig. 2. Histograms of error (%) for the I_{SC} values of the test PV modules ((a) mc-Si, (b) HIT, (c) BC, (d) CIS, and (e) CdTe modules). The I_{SC} is descripted by IrrT (model A) and $IrrT_{PVMS}$ (model B). The figures were constructed with 174,285 data points in a year with solar irradiance of ≥0 kW/m^2.

histogram, which can be explained by median and interquartile range (IQR) values, is a graphical representation of the data distribution, where the median is the value separating the higher half of data distribution from the lower half, as well as the IQR is an index of statistical dispersion, equal to the difference between 75th and 25th percentiles. It is disclosed in Fig. 2 that both median and IQR for the model B ($IrrT_{PVMS}$) are closer to zero and narrower, respectively, than those for the model A (IrrT). The result implied that the higher precision for the description of the I_{SC} using $IrrT_{PVMS}$ (model B in Equation (3)) is obtained, attributed to the $IrrT_{PVMS}$ observed by the sc-Si PV module (PVMS) with the fast measurement time and the similar AOI of sc-Si module to the test PV module. It is moreover found that the IQR values ($IrrT_{PVMS}$ or model B) of the CIS and CdTe PV modules are broader than those of the mc-Si, HIT, and BC PV modules, because the E_g values of CIS and CdTe modules in Table 1 are very different from the sc-Si PV module (PVMS). Therefore, the APE as an indicator of the solar spectral irradiance variations is added in the models C (Equation (4)) and D (Equation (5)) using $IrrT_{PVMS}$ (simultaneous solar irradiance), which will be discussed in the next section, to minimize the spectral mismatch error caused by E_g difference between the test PV module and sc-Si PV module (PVMS) for the higher precision of the I_{SC} description.

3.2. *Description of I_{SC} of test PV modules under various solar irradiance levels*

In this section, the I_{SC} of the test PV modules is descripted under different solar irradiance levels by the model B ($IrrT_{PVMS}$), model C ($IrrT_{PVMS}$, and APE) and model D ($IrrT_{PVMS}$, APE, T_{mod}) for the comparison. It is noted that T_{mod} is added in the model D to minimize the effect of the T_{mod}. It is notable that the model to precisely descript the I_{SC} under not only sunny day but also cloudy day (various solar irradiance levels) is investigated and developed, thereby enhancing the outdoor measurement opportunity.

The data points were accumulated from July 1st, 2016 to June 30th, 2017 (one year) with the total data points of 174,285 at the outdoor installation site of the test PV modules. Since the I_{SC} of the test PV modules under different solar irradiance levels were descripted, Fig. 3 illustrates the ratio of used data to the total data point multiplying 100 (%), as well as the used data point as a function of $IrrT_{PVMS}$. The used data mean that the data were utilized to descript the I_{SC} of test PV modules. It is implied that the number of data (used data points) with $IrrT_{PVMS}$ of ≥0 kW/m^2 is the largest

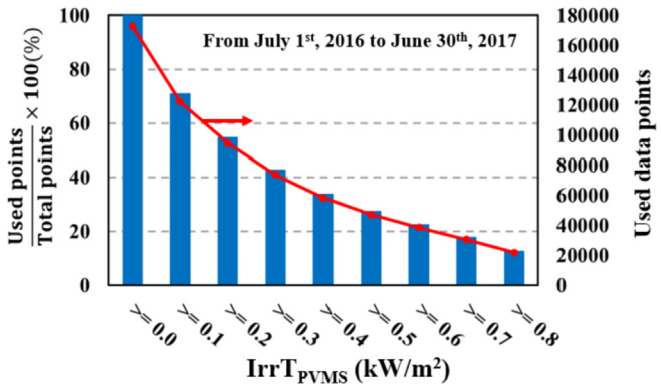

Fig. 3. Ratio of used data to the total data point multiplying 100 (%) and used data points as a function of $IrrT_{PVMS}$. The used data mean that the data were utilized to descript the I_{SC} of test PV modules. The data were accumulated from July 1st, 2016 to June 30th, 2017.

number in Fig. 3, because they are accumulated on both sunny day and cloudy day. On the other hand, the number of data (used data points) with $IrrT_{PVMS}$ of $\geq$0.8 kW/m^2 is the lowest in Fig. 3, as they are accumulated only on the sunny day.

According to the multiple regression analysis, the *b*, *c*, *d* and *e* constants (PRC) for models B ($IrrT_{PVMS}$), C ($IrrT_{PVMS}$, and APE), and D ($IrrT_{PVMS}$, APE, and T_{mod}) were first calculated based on the environmental factor ($IrrT_{PVMS}$, APE, and T_{mod}) data set with various $IrrT_{PVMS}$ values of $\geq$0, $\geq$0.1, $\geq$0.2, $\geq$0.3, $\geq$0.4, $\geq$0.5, $\geq$0.6, $\geq$0.7, and $\geq$0.8 kW/m^2 using Equations (3)–(5), respectively. The PRC values (*b*, *c*, *d*, and *e* constants) are the values to present the relationship between the I_{SC} and the environmental factors ($IrrT_{PVMS}$, APE, and T_{mod}), respectively. For the comparison, Tables 3–5 therefore show the corresponding standard partial regression coefficient values (SPRC) of the *b*, *c*, and *d* constants of the test mc-Si, HIT, BC, CIS, and CdTe PV modules to descript the I_{SC}, estimated utilizing the models B, C, and D under various $IrrT_{PVMS}$ values of $\geq$0, $\geq$0.1, $\geq$0.2, $\geq$0.3, $\geq$0.4, $\geq$0.5, $\geq$0.6, $\geq$0.7, and $\geq$0.8 kW/m^2, respectively. It is noted that the SPRC of *e* constant is not shown since it is zero. This is because I_{SC} is zero under $IrrT_{PVMS}$ of zero. It is revealed that the *b* constant (SPRC) relating to $IrrT_{PVMS}$ in Tables 3–5 is close to 1, and the *b* constant in Tables 4 and 5 is much higher than *c* and *d* constants (SPRC) for the models C and D. The results imply that the I_{SC} is primarily determined by $IrrT_{PVMS}$. According to the result, it is disclosed that the multiple regression analysis enables us to separately and quantitatively investigate how environmental factors ($IrrT_{PVMS}$, APE, and T_{mod}) are related to the I_{SC} through the SPRC (*b*, *c*, and *d* constants) by the models B, C, and D as shown in Table 3–5

Once the *b*, *c*, and *d* constants (SPRC) in Tables 3–5 are known, the estimated I_{SC} of the test PV modules under different $IrrT_{PVMS}$ levels is calculated by the models B, C, and D. Fig. 4 consequently depicts the histograms of error (%) for the I_{SC} values using models B ($IrrT_{PVMS}$), C ($IrrT_{PVMS}$, and APE), and D ($IrrT_{PVMS}$, APE, and T_{mod}) under the data with (a) $IrrT_{PVMS}$ of $\geq$0 kW/m^2 and (b) $IrrT_{PVMS}$ of $\geq$0.5 kW/m^2 for the mc-Si PV module, as well as the histograms of error (%) using models B ($IrrT_{PVMS}$), C ($IrrT_{PVMS}$, and APE), and D ($IrrT_{PVMS}$, APE, and T_{mod}) under the data with (c) $IrrT_{PVMS}$ of $\geq$0 kW/m^2 and (d) $IrrT_{PVMS}$ of $\geq$0.5 kW/m^2 for the CdTe PV module. Based on the histograms of error (%) for the I_{SC} values with different $IrrT_{PVMS}$ levels in Fig. 4, the median and IQR were calculated. As a result, Fig. 5 demonstrates the corresponding median and IQR of histograms of error (%) for the I_{SC} values using models B ($IrrT_{PVMS}$), C ($IrrT_{PVMS}$, and APE), and D ($IrrT_{PVMS}$, APE, and T_{mod}) as a function of $IrrT_{PVMS}$ ($\geq$0, $\geq$0.1, $\geq$0.2, $\geq$0.3, $\geq$0.4, $\geq$0.5, $\geq$0.6, $\geq$0.7, and $\geq$0.8 kW/m^2) for (a) mc-Si PV module and (b) CdTe PV module. The mc-Si PV module and CdTe module are observed in Figs. 4 and 5 as examples of the investigation, since the E_g of the mc-Si PV module (1.17 eV) is the closest to that (1.16 eV) of the sc-Si PV module (PVMS), while the E_g (1.47 eV) of the CdTe PV module is the most different from that of the sc-Si PV module in Table 1. It is revealed that the low medians, implying high precision, are observed in ranges of below ±0.5% for the mc-Si PV in Fig. 5(a) and below ± 1% for the CdTe PV module in Fig. 5(b) under different $IrrT_{PVMS}$ levels by the models B ($IrrT_{PVMS}$), C ($IrrT_{PVMS}$, and APE), and D ($IrrT_{PVMS}$, APE, and T_{mod}), implying that the I_{SC} is strongly affected by $IrrT_{PVMS}$. It is also found that the high precision or low median under $IrrT_{PVMS}$ of $\geq$0 kW/m^2 accumulated on both sunny day and cloudy day is realized, thereby suggesting the enhancement of the investigation opportunity by utilizing the models B, C, and D. In addition, the IQR under $IrrT_{PVMS}$ of $\geq$0 kW/m^2 by the model B ($IrrT_{PVMS}$) is the highest in the models B, C, and D, because the E_g of the test PV modules is different from that of the sc-Si PV module (PVMS) used to determine the $IrrT_{PVMS}$, leading to the spectral mismatch. The IQR under $IrrT_{PVMS}$ of $\geq$0 kW/m^2 is obviously reduced by the models C and D as compared with the model B, especially in Fig. 5(b) for the case of the CdTe PV module, whose E_g (1.47 eV) is most different from that (1.16 eV) of the sc-Si PV module (PVMS). This decreased IQR by the models C and D is attributable to the consideration of the impact of the spectral mismatch between the PVMS and the test PV modules by adding APE parameter as shown in Equation (4) for model C and Equation (5) for model D. It is moreover seen that both median and IQR are reduced with the increased $IrrT_{PVMS}$ of $\geq$0.5 kW/m^2 (on sunny day) due to the stable solar irradiance.

As demonstrated in Fig. 5, the median and IQR for the models C and D are low and almost similar under the variation of $IrrT_{PVMS}$ ($\geq$0, $\geq$0.1, $\geq$0.2, $\geq$0.3, $\geq$0.4, $\geq$0.5, $\geq$0.6, $\geq$0.7, and $\geq$0.8 kW/m^2), implying that the I_{SC} is well descripted by the models C and D. It is additionally revealed that the I_{SC} is least affected by the T_{mod}. This is because the $IrrT_{PVMS}$ is determined by the sc-Si PV module (PVMS) installed at the same outdoor location as the test PV module, thus resulting in the almost same T_{mod} between PVMS and test PV module. Moreover, the temperature coefficient (α) values for the I_{SC} of the PVMS and the test PV modules are very low and close to each other. Namely, the α values are 0.020, 0.039, 0.034, 0.035, 0.006, and 0.045%/°C for the sc-Si (PVMS), mc-Si, HIT, BC, CIS, and CdTe in Table 1, respectively.

Table 3
SPRC value (*b* constant) of the test mc-Si, HIT, BC, CIS, and CdTe PV modules to descript the I_{SC}, calculated using the model B in Equation (3) through the multiple regression analysis under different $IrrT_{PVMS}$ values of $\geq$0, $\geq$0.1, $\geq$0.2, $\geq$0.3, $\geq$0.4, $\geq$0.5, $\geq$0.6, $\geq$0.7, and $\geq$0.8 kW/m^2, respectively.

	SPRC	$IrrT_{PVMS}$ $\geq$0.0 kW/m^2	$IrrT_{PVMS}$ $\geq$0.1 kW/m^2	$IrrT_{PVMS}$ $\geq$0.2 kW/m^2	$IrrT_{PVMS}$ $\geq$0.3 kW/m^2	$IrrT_{PVMS}$ $\geq$0.4 kW/m^2	$IrrT_{PVMS}$ $\geq$0.5 kW/m^2	$IrrT_{PVMS}$ $\geq$0.6 kW/m^2	$IrrT_{PVMS}$ $\geq$0.7 kW/m^2	$IrrT_{PVMS}$ $\geq$0.8 kW/m^2
mc-Si Module	*b*	0.999	0.998	0.998	0.997	0.995	0.991	0.986	0.976	0.974
HIT Module	*b*	0.999	0.998	0.967	0.953	0.949	0.942	0.930	0.917	0.915
BC Module	*b*	0.999	0.998	0.958	0.935	0.927	0.922	0.920	0.917	0.912
CIS Module	*b*	0.995	0.994	0.958	0.949	0.933	0.929	0.923	0.915	0.908
CdTe Module	*b*	0.996	0.995	0.992	0.989	0.983	0.975	0.965	0.949	0.928

Table 4
SPRC values (*b*, and *c* constants) of the test mc-Si, HIT, BC, CIS, and CdTe PV modules to descript the I_{SC}, estimated utilizing the model C in Equation (4) under various $IrrT_{PVMS}$ values of ≥0, ≥0.1, ≥0.2, ≥0.3, ≥0.4, ≥0.5, ≥0.6, ≥0.7, and ≥0.8 kW/m^2, respectively.

	SPRC	$IrrT_{PVMS} \geq 0.0$ kW/m^2	$IrrT_{PVMS} \geq 0.1$ kW/m^2	$IrrT_{PVMS} \geq 0.2$ kW/m^2	$IrrT_{PVMS} \geq 0.3$ kW/m^2	$IrrT_{PVMS} \geq 0.4$ kW/m^2	$IrrT_{PVMS} \geq 0.5$ kW/m^2	$IrrT_{PVMS} \geq 0.6$ kW/m^2	$IrrT_{PVMS} \geq 0.7$ kW/m^2	$IrrT_{PVMS} \geq 0.8$ kW/m^2
mc-Si Module	*b*	0.999	0.999	0.999	0.997	0.994	0.990	0.983	0.973	0.971
	c	0.005	0.008	0.009	0.009	0.009	0.009	0.010	0.012	0.017
HIT Module	*b*	0.998	0.997	0.967	0.949	0.947	0.939	0.925	0.915	0.909
	c	−0.003	−0.004	−0.001	−0.002	−0.003	−0.006	−0.010	−0.013	−0.008
BC Module	*b*	0.998	0.997	0.959	0.936	0.925	0.919	0.915	0.912	0.904
	c	−0.003	−0.002	0.002	0.003	0.003	0.003	0.001	−0.001	0.002
CIS Module	*b*	0.995	0.992	0.955	0.944	0.933	0.926	0.919	0.912	0.904
	c	0.003	0.010	0.020	0.020	0.019	0.017	0.014	0.013	0.020
CdTe Module	*b*	0.999	0.999	0.999	0.992	0.979	0.964	0.948	0.929	0.912
	c	0.014	0.029	0.038	0.045	0.053	0.062	0.070	0.079	0.099

Table 5
SPRC values (*b*, *c*, and *d* constants) of the test mc-Si, HIT, BC, CIS, and CdTe PV modules to descript the I_{SC}, estimated using the model D in Equation (5) under several $IrrT_{PVMS}$ values of ≥0, ≥0.1, ≥0.2, ≥0.3, ≥0.4, ≥0.5, ≥0.6, ≥0.7, and ≥0.8 kW/m^2, respectively.

	SPRC	$IrrT_{PVMS}$ ≥0.0 kW/m^2	$IrrT_{PVMS}$ ≥0.1 kW/m^2	$IrrT_{PVMS}$ ≥0.2 kW/m^2	$IrrT_{PVMS}$ ≥0.3 kW/m^2	$IrrT_{PVMS}$ ≥0.4 kW/m^2	$IrrT_{PVMS}$ ≥0.5 kW/m^2	$IrrT_{PVMS}$ ≥0.6 kW/m^2	$IrrT_{PVMS}$ ≥0.7 kW/m^2	$IrrT_{PVMS}$ ≥0.8 kW/m^2
mc-Si Module	*b*	0.998	0.999	0.997	0.994	0.990	0.984	0.978	0.968	0.969
	c	0.004	0.007	0.007	0.006	0.004	0.002	−0.0002	−0.003	0.002
	d	0.003	0.001	0.003	0.005	0.009	0.013	0.017	0.024	0.024
HIT Module	*b*	0.996	0.994	0.964	0.944	0.938	0.931	0.922	0.914	0.904
	c	−0.004	−0.006	0.001	0.003	0.003	0.003	0.002	0.002	0.008
	d	0.002	0.005	−0.004	−0.008	−0.012	−0.016	−0.019	−0.023	−0.026
BC Module	*b*	0.999	0.990	0.960	0.936	0.922	0.917	0.914	0.911	0.903
	c	−0.004	−0.006	0.003	0.006	0.009	0.011	0.012	0.012	0.017
	d	0.007	0.010	−0.002	−0.006	−0.010	−0.014	−0.017	−0.020	−0.024
CIS Module	*b*	0.985	0.981	0.948	0.940	0.924	0.921	0.912	0.909	0.901
	c	0.003	0.004	0.039	0.043	0.041	0.041	0.038	0.035	0.036
	d	0.003	0.014	−0.038	−0.041	−0.041	−0.042	−0.040	−0.036	−0.026
CdTe Module	*b*	0.977	0.981	0.978	0.970	0.957	0.942	0.928	0.912	0.902
	c	0.008	0.017	0.021	0.023	0.025	0.025	0.022	0.019	0.026
	d	0.029	0.027	0.031	0.038	0.048	0.060	0.076	0.095	0.115

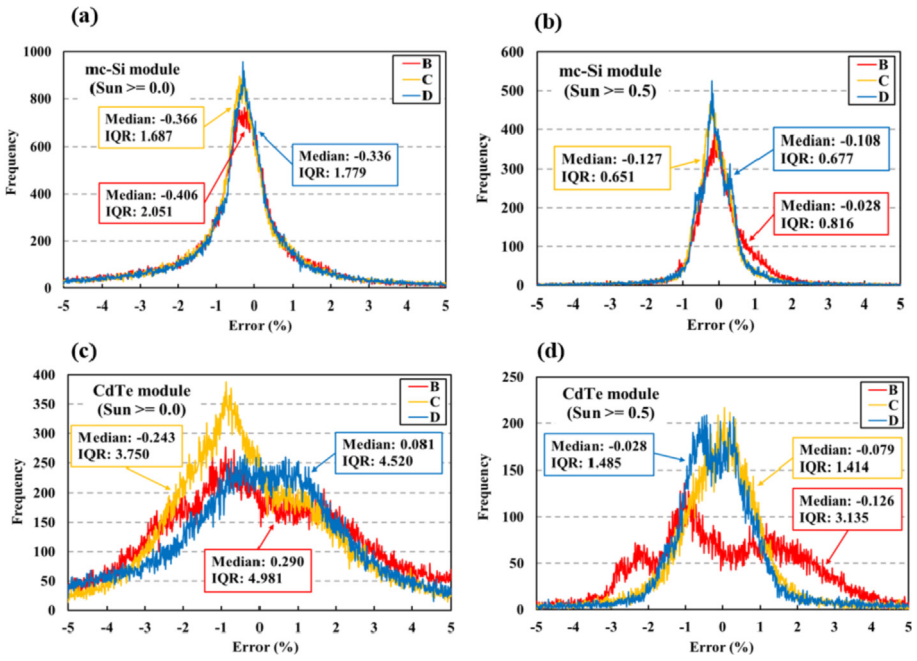

Fig. 4. Histograms of error (%) for the I_{SC} values using models B ($IrrT_{PVMS}$), C ($IrrT_{PVMS}$, and APE), and D ($IrrT_{PVMS}$, APE, and T_{mod}) under the data with (a) $IrrT_{PVMS}$ of $\geq$0 kW/m^2 and (b) $IrrT_{PVMS}$ of $\geq$0.5 kW/m^2 for the mc-Si PV module, as well as the histograms of error (%) using model B ($IrrT_{PVMS}$), C ($IrrT_{PVMS}$, and APE), and D ($IrrT_{PVMS}$, APE, and T_{mod}) under the data with (c) $IrrT_{PVMS}$ of $\geq$0 kW/m^2 and (d) $IrrT_{PVMS}$ of $\geq$0.5 kW/m^2 for the CdTe PV module.

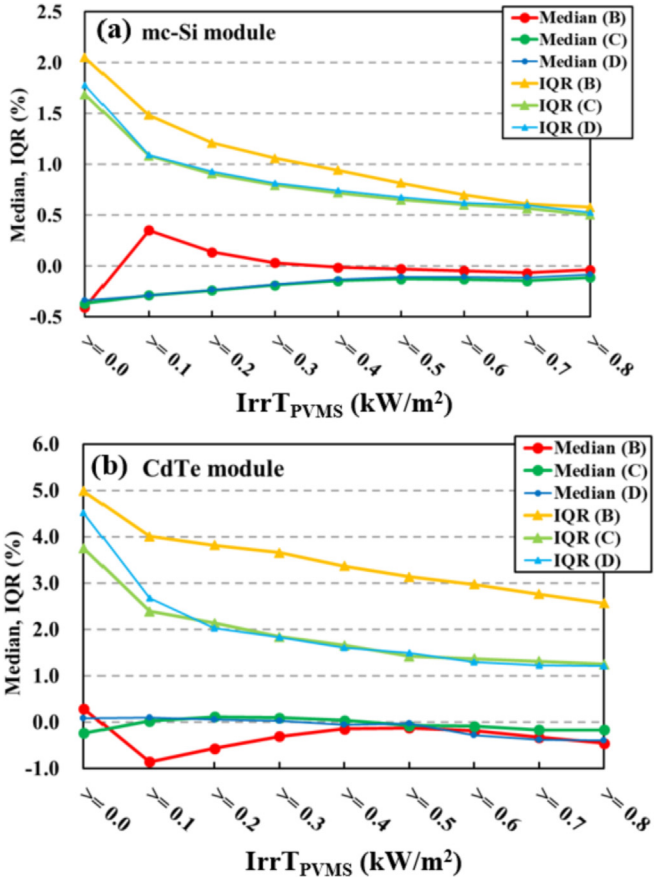

Fig. 5. Median and IQR of histograms of error (%) for the I_{SC} values using models B ($IrrT_{PVMS}$), C ($IrrT_{PVMS}$, and APE), and D ($IrrT_{PVMS}$, APE, and T_{mod}) as a function of $IrrT_{PVMS}$ ($\geq$0, $\geq$0.1, $\geq$0.2, $\geq$0.3, $\geq$0.4, $\geq$0.5, $\geq$0.6, $\geq$0.7, and $\geq$0.8 kW/m^2) for (a) the mc-Si PV module and (b) the CdTe PV module.

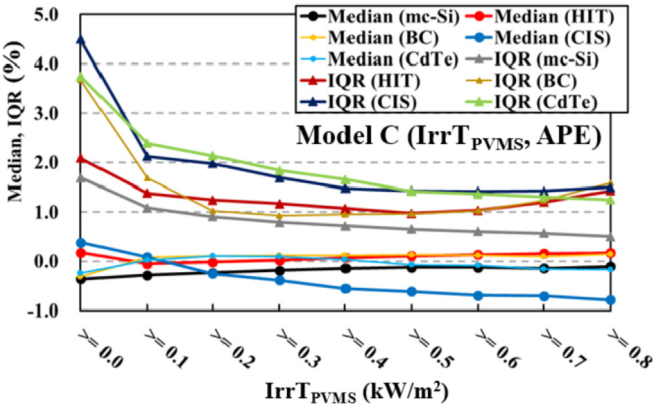

Fig. 6. Median and IQR of histograms of error (%) for the I_{SC} values using model C ($IrrT_{PVMS}$, and APE) as a function of $IrrT_{PVMS}$ ($\geq$0, $\geq$0.1, $\geq$0.2, $\geq$0.3, $\geq$0.4, $\geq$0.5, $\geq$0.6, $\geq$0.7, and $\geq$0.8 kW/m^2) for the test PV modules (mc-Si, HIT, BC, CIS, and CdTe modules).

For simplicity, the model C using $IrrT_{PVMS}$ and APE is ultimately considered to be the most suitable for the description of I_{SC}. Fig. 6 therefore illustrates the median and IQR of histograms of error (%) for the I_{SC} values using the model C ($IrrT_{PVMS}$, and APE) as a function of $IrrT_{PVMS}$ ($\geq$0, $\geq$0.1, $\geq$0.2, $\geq$0.3, $\geq$0.4, $\geq$0.5, $\geq$0.6, $\geq$0.7, and $\geq$0.8 kW/m^2) for the different-type test PV modules (mc-Si, HIT, BC, CIS, and CdTe modules). It is disclosed that the low median of below ±1% for the different-type test PV modules under different $IrrT_{PVMS}$ levels is observed, implying the high precision of the description of their I_{SC} using the model C even under $IrrT_{PVMS}$ of $\geq$0 kW/m^2, accumulated on both sunny day and cloudy day suggesting the enhancement of the investigation opportunity by the model C. Furthermore, the low IQR of below 4.5% through the model C is observed under $IrrT_{PVMS}$ of $\geq$0 kW/m^2 even in the CIS and CdTe PV modules having their E_g different from that of the sc-Si PV module (PVMS). This is because the description of I_{SC} using the

model C is considered to reduce the spectrum mismatch owing to the E_g difference by adding the APE. The IQR for all test PV modules in Fig. 6 is further decreased under the enhanced $IrrT_{PVMS}$ of $\geq$0.5 kW/m^2 (on sunny day) due to the stable solar irradiance. Ultimately, the method utilizing the model C ($IrrT_{PVMS}$, and APE) through the multiple regression analysis for the description of I_{SC} is simple and applicable to many outdoor installation sites under various solar irradiance levels.

4. Conclusions

The I_{SC} of the different-type PV modules was descripted based on the environmental factors (IrrT, $IrrT_{PVMS}$, APE, or T_{mod}) under the various solar irradiance levels by the multiple regression analysis. It is disclosed that the higher precision for the description of the I_{SC} based on $IrrT_{PVMS}$ is obtained, attributed to the $IrrT_{PVMS}$ observed by the sc-Si PV module (PVMS) with the fast measurement time and the similar AOI of the sc-Si module to the test PV modules. Moreover, from the multiple regression analysis, the I_{SC} is mainly determined by $IrrT_{PVMS}$. Ultimately, the method (model C) utilizing $IrrT_{PVMS}$ and APE environment factors through the multiple regression analysis for the description of I_{SC} is simple and applicable to many outdoor installation sites with high precision even under $IrrT_{PVMS}$ of $\geq$0 kW/m^2, thus the enhancement of the investigation opportunity. This is because $IrrT_{PVMS}$ is related to the simultaneous solar irradiance and the APE is considered to minimize the effect of E_g difference between the PVMS and test PV module (spectral mismatch). Moreover, the IQR is further decreased under the enhanced $IrrT_{PVMS}$ of $\geq$0.5 kW/m^2 (on sunny day) due to the stable solar irradiance.

Acknowledgement

This work is partly supported by the New Energy and Industrial Technology Development Organization (NEDO), Japan.

References

[1] Y. Hamakawa, Background and motivation for thin-film solar-cell development, in: Y. Hamakawa (Ed.), Thin-Film Solar Cells Next Generation Photovoltaics and its Applications, Springer, Heidelberg, 2004, pp. 1–14.
[2] E. Vallat-Sauvain, A. Shah, J. Bailat, Epitaxial thin film crystalline silicon solar cells on low cost silicon carriers, in: J. Poortmans, V. Arkhipov (Eds.), Thin Film Solar Cells, Fabrication, Characterization and Applications, Wiley, Chichester, 2006, pp. 1–32.
[3] International Electrotechnical Commission, IEC 60904-3..
[4] Japan Industrial Standard Committee, JIS C8904-3..
[5] International Electrotechnical Commission, IEC 61853-3..
[6] T. Minemoto, S. Nagae, H. Takakura, Impact of spectral irradiance distribution and temperature on the outdoor performance of amorphous Si photovoltaic modules, Sol. Energy Mater. Sol. Cells 91 (2007) 919–923.
[7] T. Minemoto, H. Takahashi, Y. Nakada, H. Takakura, Outdoor performance evaluation of photovoltaic modules using contour plots, Curr. Appl. Phys. 10 (2010) S257–S260.
[8] T. Minemoto, M. Toda, S. Nagae, M. Gotoh, A. Nakajima, K. Yamamoto, H. Takakura, Y. Hamakawa, Effect of spectral irradiance distribution on the outdoor performance of amorphous Si//thin-film crystalline Si stacked photovoltaic modules, Sol. Energy Mater. Sol. Cells 91 (2007) 120–122.
[9] S. Nagae, M. Toda, T. Minemoto, H. Takakura, Y. Hamakawa, Evaluation of the impact of solar spectrum and temperature variations on output power of silicon-based photovoltaic modules, Sol. Energy Mater. Sol. Cells 90 (2006) 3568–3575.
[10] Y. Nakada, S. Fukushige, T. Minemoto, H. Takakura, Seasonal variation analysis of the outdoor performance of amorphous Si photovoltaic modules using the contour map, Sol. Energy Mater. Sol. Cells 93 (2009) 334–337.
[11] H. Takahashi, S. Fukushige, T. Minemoto, H. Takakura, Output estimation of Si-based photovoltaic modules with outdoor environment and output map, J. Cryst. Growth 311 (2009) 749–752.
[12] T. Minemoto, Y. Nakada, H. Takahashi, H. Takakura, Uniqueness verification of solar spectrum index of average photon energy for evaluating outdoor performance of photovoltaic models, Sol. Energy 83 (2009) 1294–1299.
[13] C. Radue, E.E. van Dyk, A comparison of degradation in three amorphous silicon PV module technologies, Sol. Energy Mater. Sol. Cells 94 (2010) 617–622.
[14] P. Sanchez-Friera, M. Piliougine, J. Pelaez, J. Carretero, M.S. de Cardona, Analysis of degradation mechanisms of crystalline silicon PV modules after 12 years of operation in southern Europe, Prog. Photovolt. Res. Appl. 19 (2011) 658–666.
[15] A. Phinikarides, N. Kindyni, G. Makrides, G.E. Georghiou, Review of photovoltaic degradation rate methodologies, Renew. Sustain. Energy Rev. 40 (2014) 143–152.
[16] P. Ingenhoven, G. Belluardo, D. Moser, Comparison of statistical and deterministic smoothing methods to reduce the uncertainty of performance loss rate estimates, IEEE J. Photovolt. 8 (2018) 224–232.
[17] Y. Hishikawa, T. Doi, M. Higa, K. Yamagoe, H. Ohshima, Precise outdoor PV module performance characterization under unstable irradiance, IEEE J. Photovoltaics 6 (2016) 1221–1227.
[18] Y. Imai, J. Chantana, Y. Kawano, Y. Hishikawa, T. Minemoto, Description of performance degradation of photovoltaic modules using spectral mismatch correction factor under different irradiance levels, Renew. Energy 141 (2019) 444–450.
[19] J. Cohen, P. Cohen, S.G. West, L.S. Aiken, Applied Multiple Regression/Correlation Analysis for the Behavioral Sciences, Lawrence Eribaum Associates, Inc., New Jersey, 2003, pp. 64–99 (Chapter 3).
[20] Photovoltaic devices-Part 3: measurement principles for terrestrial photovoltaic (PV) solar devices with reference spectral irradiance data, IEC (2009), 60904-4.
[21] S.R. Williams, T.R. Betts, T. Helf, R. Gottschalg, H.G. Beyer, D.G. Infield, Modelling long-term module performance based on realistic reporting conditions with consideration to spectral effects, in: Proceedings of the 3rd World Conference on Photovoltaic Energy Conversion, 2003, pp. 1908–1911.
[22] J. Chantana, S. Ueno, Y. Ota, K. Nishioka, T. Minemoto, Uniqueness verification of direct solar spectral index for estimating outdoor performance of concentrator photovoltaic systems, Renew. Energy 75 (2015) 762–766.
[23] International Electrotechnical Commission. 2008. IEC 60904-3..
[24] Japan Industrial Standard Committee, 2011, JIS C 8904-3..
[25] C. Cornaro, A. Andreotti, Influence of average photon energy index on solar irradiance characteristics and outdoor performance of photovoltaic modules, Prog. Photovolt. Res. Appl. 21 (2013) 996–1003.
[26] A. Fukabori, T. Takenouchi, Y. Matsda, Y. Tsuno, Y. Hishikawa, Study of highly precise outdoor characterization technique for photovoltaic modules in terms of reproducibility, Jpn. J. Appl. Phys. 54 (2015), 08KG06.
[27] Y. Hishikawa, T. Doi, M. Higa, K. Yamagoe, H. Ohshima, K. Matsuda, H. Wakabayashi, Precise Outdoor PV Performance Measurements at Various Irradiance Levels, The 43rd IEEE PVSC, Porland, 2016.